Synchronization in Hindmarsh–Rose neurons subject to higher-order interactions

Cite as: Chaos **32**, 013125 (2022); doi: 10.1063/5.0079834
Submitted: 25 November 2021 · Accepted: 3 January 2022 ·
Published Online: 18 January 2022

Fatemeh Parastesh,[1] Mahtab Mehrabbeik,[1] Karthikeyan Rajagopal,[2] Sajad Jafari,[1,3] and Matjaž Perc[4,5,6,7,a)]

AFFILIATIONS

[1]Department of Biomedical Engineering, Amirkabir University of Technology (Tehran polytechnic), Tehran 159163-4311, Iran
[2]Centre for Nonlinear Systems, Chennai Institute of Technology, Tamil Nadu 600069, India
[3]Health Technology Research Institute, Amirkabir University of Technology (Tehran polytechnic), Tehran 159163-4311, Iran
[4]Faculty of Natural Sciences and Mathematics, University of Maribor, Koroška cesta 160, 2000 Maribor, Slovenia
[5]Department of Medical Research, China Medical University Hospital, China Medical University, Taichung 404332, Taiwan
[6]Alma Mater Europaea, Slovenska ulica 17, 2000 Maribor, Slovenia
[7]Complexity Science Hub Vienna, Josefstädterstraße 39, 1080 Vienna, Austria

Note: This article is part of the Focus Issue, Dynamics on Networks with Higher-Order Interactions.
[a)]**Author to whom correspondence should be addressed:** matjaz.perc@gmail.com

ABSTRACT

Higher-order interactions might play a significant role in the collective dynamics of the brain. With this motivation, we here consider a simplicial complex of neurons, in particular, studying the effects of pairwise and three-body interactions on the emergence of synchronization. We assume pairwise interactions to be mediated through electrical synapses, while for second-order interactions, we separately study diffusive coupling and nonlinear chemical coupling. For all the considered cases, we derive the necessary conditions for synchronization by means of linear stability analysis, and we compute the synchronization errors numerically. Our research shows that the second-order interactions, even if of weak strength, can lead to synchronization under significantly lower first-order coupling strengths. Moreover, the overall synchronization cost is reduced due to the introduction of three-body interactions if compared to pairwise interactions.

Synchronous behavior in complex networks is often directly related to the type of interactions between the different components. It has recently been pointed out that the consideration of only pairwise interactions is an over-simplification for many real networks, including the nervous system. Indeed, non-pairwise interactions can have major influences on the behavior of such networks. Despite numerous studies on the synchronization of neurons subject to pairwise interactions, higher-order interactions and their impact on the emergence of synchronization are still poorly understood. To do away with this gap, we consider a simplicial complex of Hindmarsh–Rose neurons, where the impact of higher-order interactions can be studied. For pairwise interactions, we, therefore, consider only diffusive electrical synapses, while for higher-order interactions, we consider both diffusive and chemical synapses. We determine the required first- and second-order coupling strengths for synchronization by means of linear stability analysis, and we find that second-order interactions, along with pairwise electrical synapses, decrease the electrical coupling strength needed for synchronization. We also define and compute the synchronization cost for different interaction types, observing that taking into account second-order diffusive interactions reduces the cost, while second-order chemical interactions increase it. Nonetheless, the cost of second-order chemical synapses is still lower than the cost associated with first-order chemical synapses. Taken together, these results indicate a prominent role of higher-order interactions in the onset of neuronal synchronization.

I. INTRODUCTION

Complex networks are a set of nodes with specific dynamics connected by links.[1] Synchronization is among the most fascinating collective behaviors in complex networks with application in

different subjects, including technology and biology.[2] This phenomenon is referred to as the existence of common dynamics between network systems that can be coupled linearly or nonlinearly.[3] Synchronization plays a vital role in the brain activities such as the human memory process. This has been confirmed in the investigations of electroencephalography and magnetoencephalography signals.[4] Using these signals, complex networks can be constructed and analyzed.[5] Moreover, many studies can be found discussing the association between synchronization and some diseases, such as Parkinson's,[6] Alzheimer's,[7] epilepsy,[8] and autism.[9]

Due to the importance of synchronization, many researchers have investigated synchronization in neuronal networks. These studies represent the effects of different factors on the neuron's synchronization, including the coupling, topology, neuron's dynamics, time delay, and noise.[10–15] Bandyopadhyay and Kar[14] considered the Hindmarsh–Rose neurons in different network structures and focused on the synchronization problem. They found that the network with a high clustering coefficient and neutral degree mixing pattern provides a better synchronization. Rakshit *et al.*[16] examined the synchronization of neurons in a hypernetwork with time-varying links. They reported that the synchronization is enhanced in higher rewiring frequencies. Wang *et al.*[17] revealed the effects of the synaptic time delay and also self-time delay on the synchronization of neurons in a multilayer structure. The type of synapses is another factor impacting the collective behavior of the neurons. In this regard, several studies have considered electrical, chemical, and memristor-based synapses or a combination of them.[18–20]

Despite the real-world application of custom networks with dyadic interactions, it has been proved that sometimes these pairwise interactions are not satisfactory in modeling special systems, such as biological ones.[21–23] The importance of higher-order interactions in brain networks can be found in Refs. 24 and 25. These higher-order structures are called "simplicial complexes" that describe many-body interactions between network units.[26–28] According to the definition of simplicial complexes, the interaction between n+1 agents can be represented by n-simplex.[29,30] Recently, simplicial complexes have grabbed researchers' attention.[31–34] For example, Millán *et al.*[35] studied the dynamics of Kuramoto oscillators in 2-simplex structures and revealed the emergence of explosive synchronization. Additionally, they studied the effect of simplicial geometry on the phase diagram of the network of higher-order Kuramoto oscillators. Another study on higher-order phase oscillators was conducted by Skardal and Arenas,[36] which showed that by increasing the nonlinearity, the higher-order interactions lead to a self-organized feature, resulting in the rapid switching to the synchronization. The synchronization of Kuramoto oscillators was also studied by Lucas *et al.*[37] They proposed a multi-order Laplacian framework, a generalization pairwise Laplacian framework, obtained by the Lyapunov exponents. The stability of synchronization in hypernetworks has been investigated in some research studies.[38,39] Also, the study of master stability function (MSF) of higher-order interactions was conducted by Gambuzza *et al.*[40] They proposed the method for calculating the MSF of a network with many-body interactions and applied their method to the Rössler and Lorenz systems.

The investigation of higher-order interactions has not been limited to phase oscillators. The neuronal models have also been employed to study the effect of many-body interactions on their behavior. For instance, a network of Morris–Lecar neurons with higher-order interactions was studied by Tlaie *et al.*[41] Based on this study, higher-order interactions can lead to time-ordered synchronization by only a small coupling strength and provide fast information propagation. Ince *et al.*[42] also announced that pairwise interactions could not fully describe the behavior of the neurons in the rat somatosensory cortex. They also calculated the Shannon energy as a measure of transmitted information amount of the neuron's activity to evaluate the effect of higher-order interactions on the information transmission. The study conducted by Amari *et al.*[43] proved that higher-order interactions exist in neuronal activity. They showed that the generation of a widespread distribution could be due to the many-body interactions in a pool of neurons.

In this paper, the synchronization of the Hindmarsh–Rose neurons with higher-order interactions in the global coupling scheme is studied. The first-order interactions are defined by electrical gap junctions, while the second-order (or three-body) interactions are considered in two conditions: linear diffusive coupling (similar to the electrical synapses) and nonlinear chemical synaptic couplings. The linear stability analysis is done, and the required coupling strengths for synchronization are obtained. The synchronization of the neurons is also computed numerically. A synchronization cost is also introduced and computed for different connections. The results represent the enhancement of synchrony in the presence of second-order interactions.

The paper is organized as follows. Section II elaborates on the studied model. The results of two different cases of second-order interactions are detailed in Sec. III, and Sec. IV highlights the main results as the conclusion.

II. MATHEMATICAL MODEL

The simplicial complex of order D lets for considering not only pairwise connections (1-simplex known as the links) but also higher-order interactions such as the three-body interaction known as the triangles (2-simplex), four-body interaction (3-simplex), etc. Here, we consider that the neurons evolve through the first-order and second-order interactions. A simplicial complex of the order $D = 2$ is described by the following equations:

$$\dot{X} = F(X) + \sigma_1 \sum_{j=1}^{N} a_{ij}^{(1)} g_1(X_i, X_j) + \sum_{j=1}^{N} \sum_{k=1}^{N} a_{ijk}^{(2)} g_2(X_i, X_j, X_k), \quad (1)$$

where $X \in \mathbb{R}^m$ is the m-dimensional state variable of the system, $F(X) : \mathbb{R}^m \to \mathbb{R}^m$ describes the dynamical function of the nodes, and σ_1 and σ_2 are the coupling strengths of the first-order and second-order interactions. The coupling function between the nodes is defined by the matrix function $g_1(X_i, X_j)$ for 1-simplexes and by $g_2(X_i, X_j, X_k)$ for 2-simplexes. The matrix $A^{(1)} = \left[a_{ij}^{(1)}\right]$ is the first-order adjacency matrix that represents the existence of the link between nodes i and j by $a_{ij}^{(1)} = 1$, and otherwise $a_{ij}^{(1)} = 0$. Similarly, $A^{(2)} = \left[a_{ijk}^{(2)}\right]$ is the adjacency tensor that refers to the 2-simplexes where $a_{ijk}^{(2)} = 1$ shows that the nodes i,j,k construct a triangle.

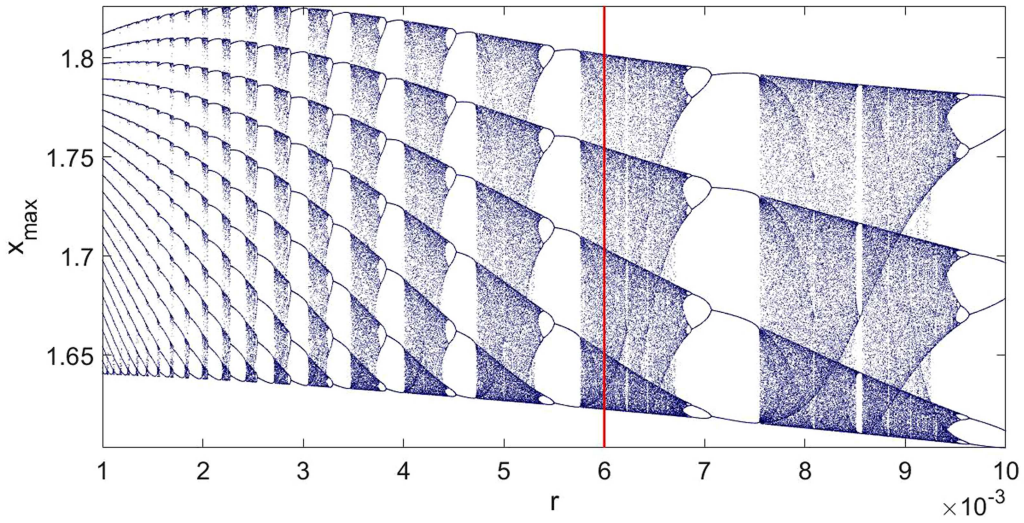

FIG. 1. Bifurcation diagram of the Hindmarsh–Rose model [Eq. (2)] according to parameter r. The model shows an intermittency between period-5 and chaotic dynamics at $r = 0.006$. Other parameters of the model are $s = 4$ and $I_{ext} = 3.2$.

Here, the three-variable Hindmarsh–Rose model ($X = [x, y, z]$) is considered to describe the dynamics of the neurons; therefore,

$$F(X) = \begin{cases} f(x,y,z) = y + 3x^2 - x^3 - z + I_{ext}, \\ g(x,y,z) = 1 - 5x^2 - y, \\ h(x,y,z) = r(s(x + 1.6) - z), \end{cases} \tag{2}$$

where x, y, and z denote the membrane potential, fast, and slow recovery variables, respectively. The parameters of the model are set at $r = 0.006$, $s = 4$, and $I_{ext} = 3.2$, where the behavior of the neuron is spike bursting.[44] The bifurcation diagram of the model according to parameter r is depicted in Fig. 1. It can be observed that the model exhibits intermittency between period-5 and chaotic

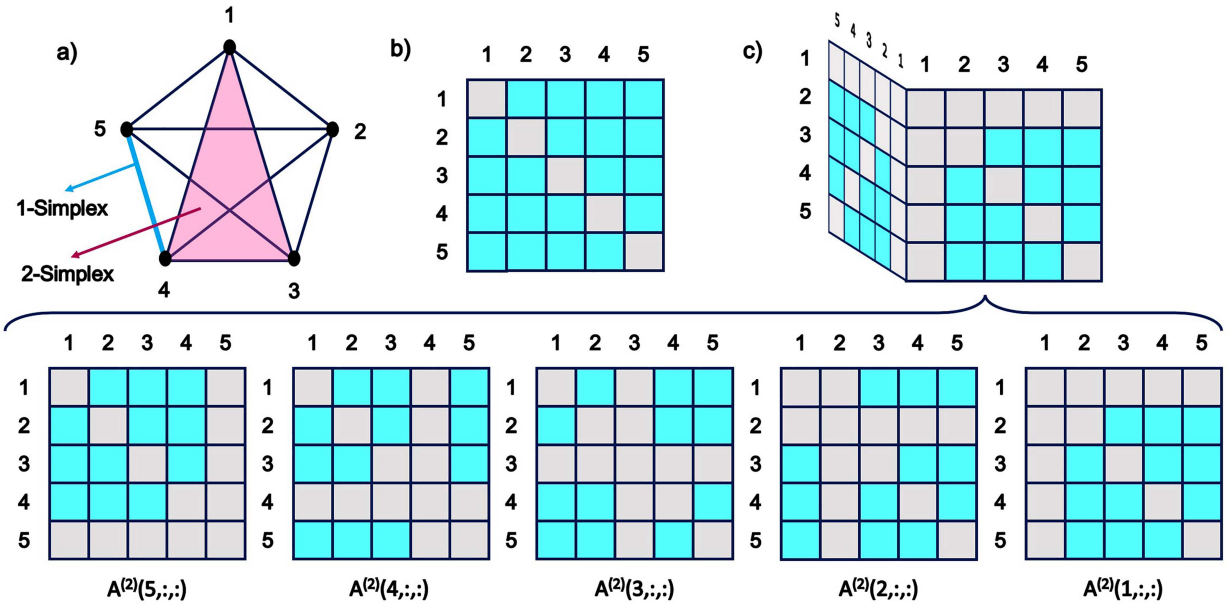

FIG. 2. (a) The schematic of a simplicial complex of five nodes with global coupling. A 1-simplex (link) and a 2-simplex (triangle) of the network are shown by blue and pink colors as an example. (b) The corresponding adjacency matrix $A^{(1)}$. The elements shown by cyan color represent a link between nodes i and j. (c) The corresponding adjacency tensor $A^{(2)}$, which is three-dimensional. The cyan elements show that the nodes i, j, k construct a triangle.

dynamics. Further, it is assumed that the neurons are connected with the global coupling configuration (all to all coupling). A schematic of the network is shown in Fig. 2(a). As an illustration, a link (1-simplex) and a triangle (2-simplex) are shown in blue and pink colors, respectively. The first- and second-order adjacency tensors are represented in Figs. 2(b) and 2(c), respectively.

III. RESULTS

The synchronization of the network of $N = 20$ neurons is investigated for different first-order and second-order coupling strengths. We consider that the first-order communication of the neurons is diffusive to describe the electrical gap junction. Therefore,

$$g_1(X_i, X_j) = [x_j - x_i, 0, 0]. \tag{3}$$

For the second-order interactions, we consider two different cases: (1) linear diffusive coupling similar to the electrical synapses and (2) nonlinear coupling raised from chemical synapses. For each case, we investigate the stability of the synchronization of the neurons by using the linear stability analysis. Therefore, the master stability function, which gives the necessary conditions for the synchronization of coupled oscillators, is derived.[40] Moreover, to evaluate the synchrony level of the neurons, the averaged synchronization error is also computed with the following equation:

$$E = \left\langle \frac{1}{N-1} \sum_{j=2}^{N} \left\| X_1(t) - X_j(t) \right\| \right\rangle_t. \tag{4}$$

A. Diffusive second-order interactions

In the first step, the second-order interactions are also considered diffusive. Thus, the function $g_2(X_i, X_j, X_k)$ is defined as follows:

$$g_2(X_i, X_j, X_k) = [x_j + x_k - 2x_i, 0, 0]. \tag{5}$$

To find the stability of the synchronization, the linear stability analysis is done on the network equation [Eq. (1)] by adding a small perturbation to the synchronous manifold X_s as $\delta X_i = X_i - X_s$, $(\delta x_i = x_i - x_s, \delta y_i = y_i - y_s, \delta z_i = z_i - z_s])$. Thus,

$$\begin{aligned}
\delta \dot{X}_i = {} & JF(X_s)\delta X_i + \sigma_1 \sum_{j=1}^{N} a_{ij}^{(1)} \\
& \times \left[\frac{\partial g_1(X_i, X_j)}{\partial X_i}\bigg|_{(X_s, X_s)} \delta X_i + \frac{\partial g_1(X_i, X_j)}{\partial X_j}\bigg|_{(X_s, X_s)} \delta X_j \right] \\
& + \sigma_2 \sum_{j=1}^{N} \sum_{k=1}^{N} a_{ijk}^{(2)} \left[\frac{\partial g_2(X_i, X_j, X_k)}{\partial X_i}\bigg|_{(X_s, X_s, X_s)} \delta X_i \right. \\
& + \frac{\partial g_2(X_i, X_j, X_k)}{\partial X_j}\bigg|_{(X_s, X_s, X_s)} \delta X_j \\
& \left. + \frac{\partial g_2(X_i, X_j, X_k)}{\partial X_k}\bigg|_{(X_s, X_s, X_s)} \delta X_k \right],
\end{aligned} \tag{6}$$

where $JF(X_s)$ denotes the Jacobean of the function $F(X)$ at the synchronous manifold X_s. In the synchronization state, $g_1(X_i, X_j) \equiv 0$, and $g_2(X_i, X_j, X_k) \equiv 0$; thus, the synchronization manifold is as follows:

$$\begin{cases}
\dot{x}_s = y_s + 3x_s^2 - x_s^3 - z_s + I_{ext}, \\
\dot{y}_s = 1 - 5x_s^2 - y_s, \\
\dot{z}_s = r(s(x_s + 1.6) - z_s),
\end{cases} \tag{7}$$

which evolves temporally the same as the single neuron. The time series and the attractor of the synchronous manifold are shown in

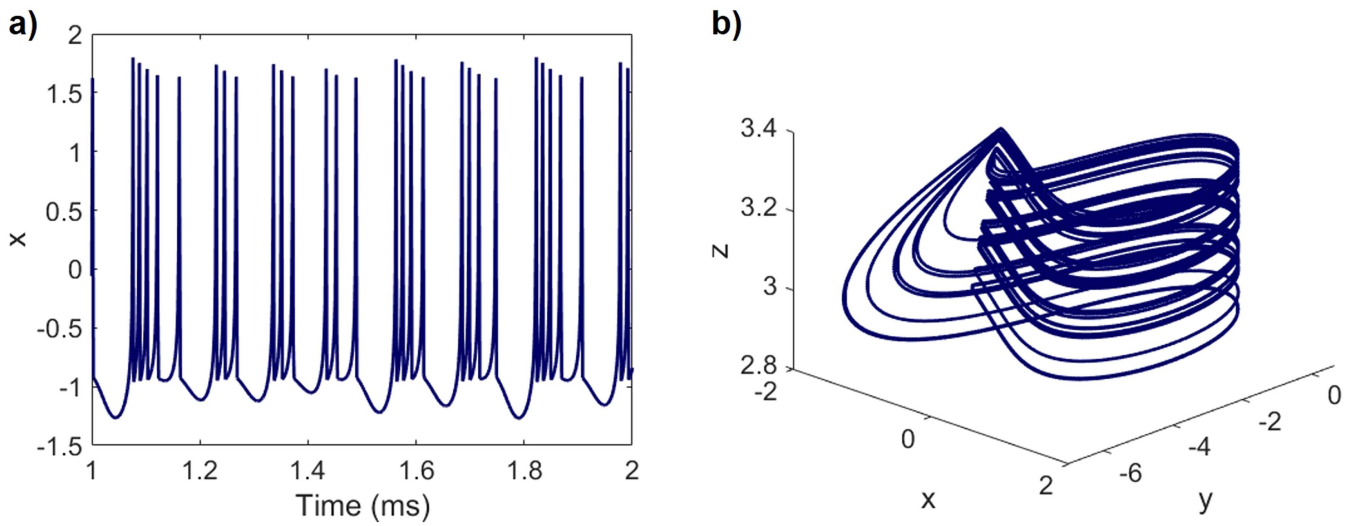

FIG. 3. The time series (a) and attractor (b) of the synchronous manifold of neurons with linear diffusive second-order interactions. The evolution of the neurons in this case is the same as the single neuron since $g_1(X_i, X_j) \equiv 0$, and $g_2(X_i, X_j, X_k) \equiv 0$ in the synchronous manifold. Therefore, the neurons have a chaotic behavior when synchronized.

Fig. 3. By considering g_1 as Eq. (3) and g_2 as Eq. (5), we can write Eq. (6) as

$$\delta\dot{x}_i = Jf(X_s)\delta X_i + \sigma_1 \sum_{j=1}^{N} a_{ij}^{(1)} \left[\delta x_j - \delta x_j\right] + \sigma_2 \sum_{j=1}^{N}\sum_{k=1}^{N} a_{ijk}^{(2)} \left[-2\delta x_i + \delta x_j + \delta x_k\right], \tag{8.1}$$

$$\delta\dot{y}_i = Jg(X_s)\delta X_i, \tag{8.2}$$

$$\delta\dot{z}_i = Jh(X_s)\delta X_i. \tag{8.3}$$

The Laplacian matrix is generally defined as $L = K - A$, where K is the diagonal matrix with the degree of the nodes at its main diagonal and A is the adjacency matrix. For our simplicial complex, the first-order Laplacian matrix $L^{(1)}$ is the classical Laplacian matrix, and the second-order one can be found as follows:

$$L_{ij}^{(2)} = \begin{cases} i \neq j : \begin{cases} a_{ij}^{(1)} = 0 : 0, \\ a_{ij}^{(1)} = 1 : -k_{ij}^{(2)}, \end{cases} \\ i = j : 2k_i^{(2)}, \end{cases} \tag{9}$$

where $k_i^{(2)} = \frac{1}{2}\sum_{j=1}^{N}\sum_{k=1}^{N} a_{ijk}^{(2)}$ is the degree of node i, and $k_{ij}^{(2)}$ is the degree of the link ij, i.e., the number of the triangles in which the link ij participates. Now, a tensor $T = \left[\tau_{ijk}\right]_{N\times N\times N}$ is introduced as $T = K^{(2)} - A^{(2)}$, where the elements of $K^{(2)}$ are $\kappa_{ijk} = 2k_i^{(2)}$ for $i = j = k$, and $\kappa_{ijk} = 0$ otherwise. Therefore, Eq. (8.1) can be rewritten as

$$\begin{aligned}
\delta\dot{x}_i &= Jf(X_s)\delta X_i - \sigma_1 \sum_{j=1}^{N} L_{ij}^{(1)}\delta x_j \\
&\quad + \sigma_2 \sum_{j=1}^{N}\sum_{k=1}^{N} \left[\kappa_{ijk} - \tau_{ijk}\right]\left[-2\delta x_i + \delta x_j + \delta x_k\right] \\
&= Jf(X_s)\delta X_i - \sigma_1 \sum_{j=1}^{N} L_{ij}^{(1)}\delta x_j - \sigma_2 \sum_{j=1}^{N}\sum_{k=1}^{N} \tau_{ijk}\left[\delta x_j + \delta x_k\right] \\
&= Jf(X_s)\delta X_i - \sigma_1 \sum_{j=1}^{N} L_{ij}^{(1)}\delta x_j \\
&\quad - \sigma_2 \left(\sum_{j=1}^{N}\delta x_j \sum_{k=1}^{N}\tau_{ijk} + \sum_{k=1}^{N}\delta x_k \sum_{j=1}^{N}\tau_{ijk}\right) \\
&= Jf(X_s)\delta X_i - \sigma_1 \sum_{j=1}^{N} L_{ij}^{(1)}\delta x_j - 2\sigma_2 \sum_{j=1}^{N} L_{ij}^{(2)}\delta x_j.
\end{aligned} \tag{10}$$

In our network, since the coupling is considered to be global, we have $L^{(2)} = (N-2)L^{(1)}$; thus,

$$\delta\dot{x}_i = Jf(X_s)\delta X_i - (\sigma_1 + 2\sigma_2 (N-2)) \sum_{j=1}^{N} L_{ij}^{(1)}\delta x_j. \tag{11}$$

Since $Jf(X_s)\delta X_i$ is the block diagonal, and the Laplacian matrix is diagonalizable, Eq. (11) can be rewritten with the eigenvalues of the Laplacian matrix. Hence, the perturbation equations [Eqs. (8.2), (8.3), and (11)] can be projected to the following linearized system with variables $\eta = [\eta_x, \eta_y, \eta_z]$ as

$$\begin{aligned}
\dot{\eta}_x &= Jf(X_s)\eta - (\sigma_1 + 2\sigma_2 (N-2))\,\lambda_i\eta_x, \\
\dot{\eta}_y &= Jg(X_s)\eta, \\
\dot{\eta}_z &= Jh(X_s)\eta,
\end{aligned} \tag{12}$$

where λ_i, $i = 1, \ldots, N$ are the eigenvalues of $L^{(1)}$. Due to the global connection matrix, $\lambda_1 = 0$ and $\lambda_i = N$ for $i = 2, \ldots, N$. For the first eigenvalue, i.e., $\lambda_1 = 0$, the system evolution is along the synchronization manifold. For other eigenvalues $\lambda_2, \ldots, \lambda_N$, the system evolution is transverse to the synchronization manifold, whose stability should be checked by calculating the maximum Lyapunov exponent (Λ). Therefore, if $\Lambda < 0$ for $\lambda = N$, then the synchronization is stable.

The maximum Lyapunov exponent of the linearized equation [Eq. (12)] for $\lambda = N = 20$ is illustrated in Fig. 4(a) according to both coupling strengths. Generally, it can be attained that with considering the second-order interactions, the synchronization is achieved in smaller coupling strength σ_1. Furthermore, this threshold is decreased with increasing the strength of the second-order interactions. The curves of Λ for different second-order coupling strength (σ_2) are plotted in Fig. 4(b) according to the first-order coupling strength (σ_1). It can be observed that in the absence of the second-order interactions, the neurons become synchronous for $\sigma_1 > 0.047$. By considering the second-order interactions, this threshold is considerably reduced even for very small σ_2. For example, for $\sigma_2 = 0.000\,15$ and $\sigma_2 = 0.0003$, the synchrony is obtained for $\sigma_1 = 0.042$ and $\sigma_1 = 0.037$, respectively. Also, it can be seen that the neurons are synchronized for any value of σ_1 when $\sigma_2 = 0.0015$. From Figs. 4(a) and 4(c), it can be seen that the border, which separates the regions of synchronization and asynchronization is a straight line. The equation of this line can be obtained from the linearized system [Eq. (12)]. As mentioned, with first-order interactions, the synchronization is stable for the coupling strengths higher than 0.047. Therefore, according to Eq. (12), $\sigma_1 + 2\sigma_2(N-2) = \sigma_1 + 36\sigma_2$ should be higher than 0.047. Thus, the equation of the borderline of synchrony and asynchrony is $\sigma_1 + 36\sigma_2 = 0.047$. In fact, for $\sigma_1 = 0$, i.e., with only considering the second-order interactions, the synchronization is achieved for $\sigma_2 > 0.0013$. From the equation of the borderline, it can be seen that σ_2 is effective with a factor of $2(N-2)$. Therefore, in second-order interactions, the synchrony can be obtained in remarkably smaller coupling strengths than the first-order interactions. The numerical synchronization error of the neurons is also represented in parts c and d, which are well-matched with the results of linear stability analysis.

Another important factor in the required coupling strength for synchronization is the considered N, i.e., the number of neurons in the network. In the absence of the second-order interactions, by increasing N, the eigenvalue of the connection matrix increases, and consequently, a lower coupling strength can synchronize the neurons. In other words, the coupling strength thresholds for synchrony in two networks with a different number of nodes have this relation:

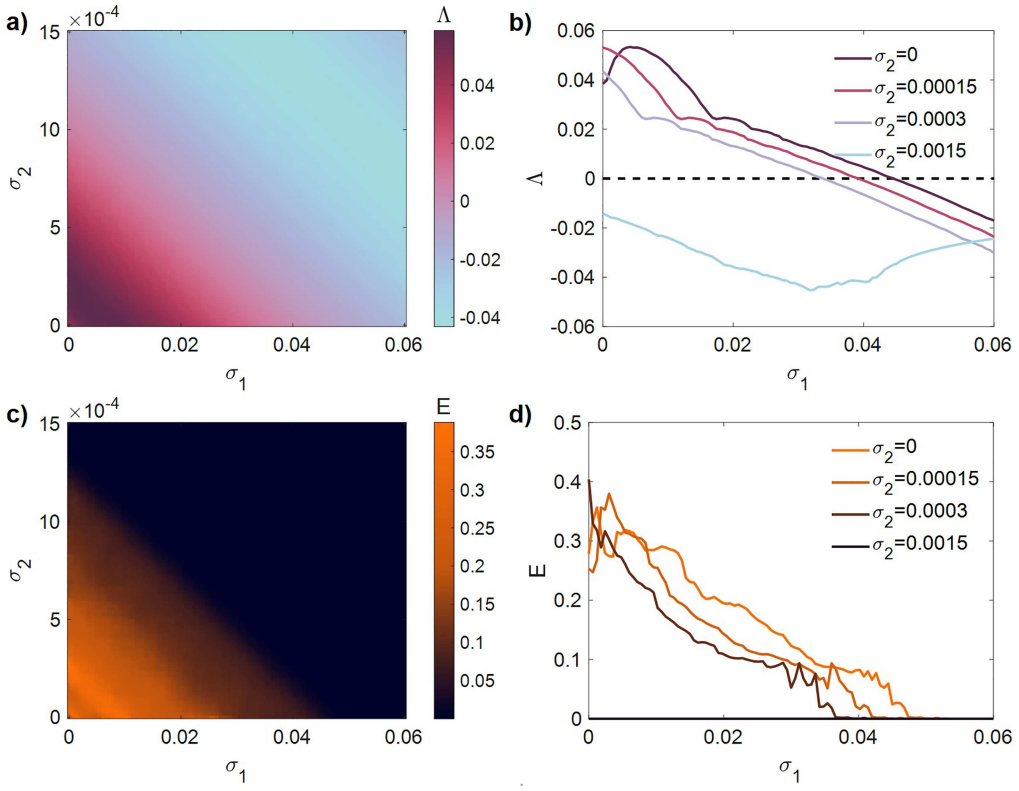

FIG. 4. The regions of synchronous and asynchronous states for $N = 20$ neurons with diffusive second-order interactions. First row: the maximum Lyapunov exponent Λ of the linearized equation (12). Second row: the synchronization error (E) computed numerically. (a) and (c) 2D representation in the parameter plane (σ_1, σ_2); the synchronous and asynchronous regions can be separated by the line: $\sigma_1 + 2\sigma_2(N-2) = \sigma_1 + 36\sigma_2 = \sigma_{th}$, where $\sigma_{th} = 0.047$ is the threshold of coupling strength for synchrony in the absence of second-order interactions. (b) and (d) 1D representation according to σ_1 for $\sigma_2 = 0, 0.000\,15, 0.0003, 0.0015$. It is clear that with increasing σ_2, the synchronization is achieved in lower σ_1.

$\frac{\sigma_1}{\sigma_1'} = \frac{N'}{N}$. On the other hand, with only considering the second-order interactions, the relation between synchrony thresholds changes to $\frac{\sigma_2}{\sigma_2'} = \frac{N'(N'-2)}{N(N-2)}$. This means that the variations in the synchrony thresholds in the second-order interaction are also affected by the coefficient $\frac{(N'-2)}{(N-2)}$. Therefore, with increasing N, the required second-order coupling strength is much more decreased. As an illustration, the regions of synchronous and asynchronous states for the network with $N = 50$ and $N = 100$ neurons are depicted in Fig. 5, which are obtained by calculating the maximum Lyapunov exponent of Eq. (12). Note the coupling ranges in these figures. The borderlines separating the regions are $\sigma_1 + 96\sigma_2 = 0.0188$ for $N = 50$ and $\sigma_1 + 196\sigma_2 = 0.0094$ for $N = 100$.

As discussed, by considering the second-order interactions, a very small σ_2 can reduce the required σ_1 for synchrony considerably. But the question is whether the second-order interactions help in enhancing synchrony or not. To answer this question, we define a synchronization cost as $C = (n_l \times \sigma_1) + (3n_t \times \sigma_2)$, where n_l is the number of the links and n_t is the number of the triangles in the network. The synchronization cost of the network in the absence ($\sigma_2 = 0$) and presence ($\sigma_1 \neq 0$) of second-order interactions is compared. In our network, the coupling is global; thus, we have $n_l = \frac{N(N-1)}{2}$ and $n_t = \frac{N(N-1)(N-2)}{6}$. When $\sigma_2 = 0$, the cost is $C_1 = \frac{N(N-1)}{2} \times \sigma_{th}$, where σ_{th} is the necessary σ_1 for synchronization when $\sigma_2 = 0$, which is $\sigma_{th} = 0.047$ for $N = 20$. By considering $\sigma_2 \neq 0$, the cost is obtained by $C_2 = \left(\frac{N(N-1)}{2} \times \sigma_1\right) + \left(\frac{3N(N-1)(N-2)}{6} \times \sigma_2\right)$. According to Eq. (12), in the synchronous state, we have $\sigma_1 + 2\sigma_2(N-2) = \sigma_{th}$ or $\sigma_2 = \frac{\sigma_{th} - \sigma_1}{2(N-2)}$. Thus,

$$C_2 = \left(\frac{N(N-1)}{2} \times \sigma_1\right) + \left(\frac{3N(N-1)(N-2)}{6} \times \frac{\sigma_{th} - \sigma_1}{2(N-2)}\right) = \frac{N(N-1)}{2}\left(\frac{\sigma_1 + \sigma_{th}}{2}\right). \quad (13)$$

As shown in Fig. 4, in the synchronous state, $\sigma_1 < \sigma_{th}$; therefore, $\frac{\sigma_1 + \sigma_{th}}{2} < \sigma_{th}$ and $C_2 < C_1$. Consequently, by incorporating the second-order interactions, the synchronization cost decreases linearly according to σ_1.

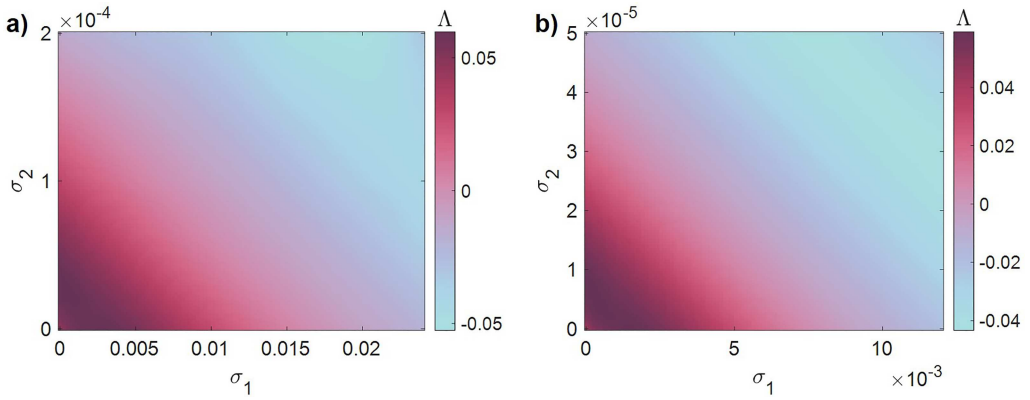

FIG. 5. The maximum Lyapunov exponent (Λ) of the linearized equation (12) for neurons with diffusive second-order interactions in the parameter plane (σ_1, σ_2) for $N = 50$ (a) and $N = 100$ (b). By increasing N to N', the first-order coupling strength decreases by the order N/N', and the second-order coupling strength decreases by the order $(N(N-2))/(N'(N'-2))$.

B. Chemical second-order interactions

In this subsection, the second-order interactions are assumed to be through chemical synapses. To this aim, the function $g_2(X_i, X_j, X_k)$ is considered as

$$g_2(X_i, X_j, X_k) = \left[(v_s - x_i)\left(\Gamma(x_j) + \Gamma(x_k)\right), 0, 0\right], \qquad (14)$$

where $\Gamma(x) = \frac{1}{1+\exp -\lambda(x-\theta_s)}$ defines the activation and deactivation of the chemical synapse with the parameters $\theta_s = -0.25$ and $\lambda = 10$, and $v_s = 2$ is the reversal potential. In this case, in the synchronization state, the second-order coupling function is $g_2(X_s, X_s, X_s) = [2(v_s - x_s)\Gamma(x_s), 0, 0]$, which is not equal to zero. Therefore, the synchronous manifold is attained as

$$\begin{cases} \dot{x}_s = ys + 3x_s^2 - x_s^3 - z_s + I_{ext} + 2\sigma_2(v_s - x_s)\Gamma(x_s), \\ \dot{y}_s = 1 - 5x_s^2 - y_s, \\ \dot{z}_s = r(s(x_s + 1.6) - z_s). \end{cases} \qquad (15)$$

Consequently, the synchronous manifold, in this case, differs from the manifold of a single neuron. The time series and attractor of this synchrony manifold [Eq. (15)] are shown in Fig. 6.

To obtain the synchronization stability for second-order chemical interactions, we rewrite the perturbation equation $\delta\dot{x}_i$ [Eq. (8.1)]

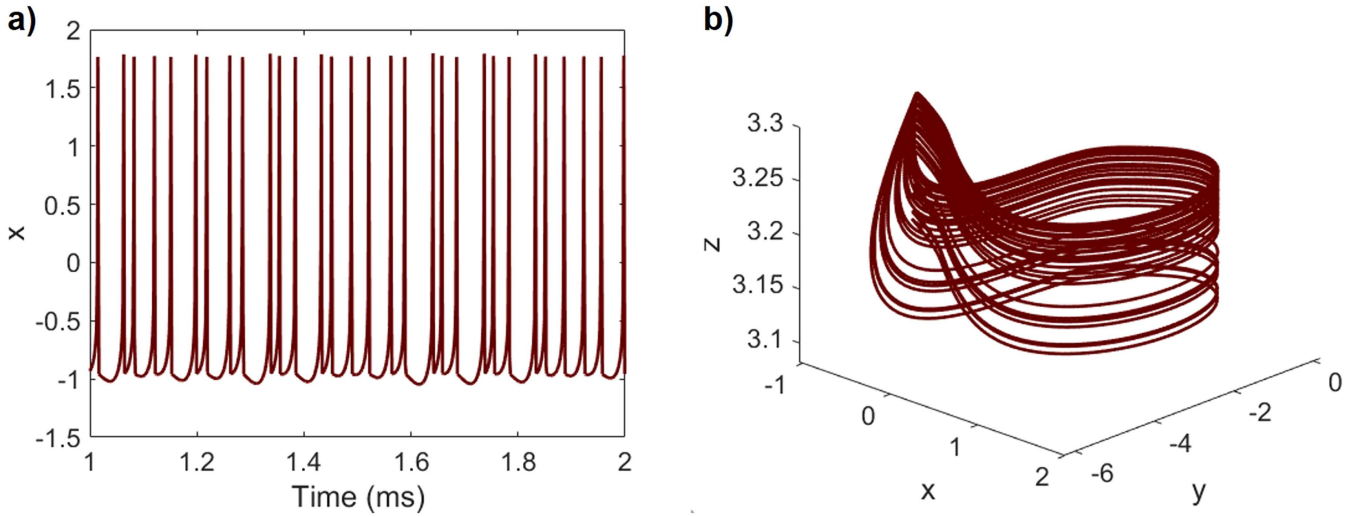

FIG. 6. The time series (a) and attractor (b) of the synchronous manifold of neurons with nonlinear chemical second-order interactions. In the synchronization manifold, the coupling term is $g_2(X_s, X_s, X_s) = [2(v_s - x_s)\Gamma(x_s), 0, 0]$, which is not equal to zero. Therefore, the evolution of neurons differs from the single neuron. However, the neurons have a chaotic firing pattern.

by using Eq. (14),

$$\begin{aligned}\delta\dot{x}_i &= Jf(X_s)\delta X_i + \sigma_1 \sum_{j=1}^{N} a_{ij}^{(1)} \left[-\delta x_i + \delta x_j\right] + \sigma_2 \sum_{j=1}^{N}\sum_{k=1}^{N} a_{ijk}^{(2)} \\ &\times \left[-2\Gamma(x_s)\delta x_i + (v_s - x_s)\,\Gamma_x(x_s)\delta x_j + (v_s - x_s)\,\Gamma_x(x_s)\delta x_k\right] \\ &= Jf(X_s)\delta X_i - \sigma_1 \sum_{j=1}^{N} L_{ij}^{(1)}\delta x_j - 2\sigma_2\Gamma(x_s)\delta x_i \sum_{j=1}^{N}\sum_{k=1}^{N} a_{ijk}^{(2)} \\ &+ \sigma_2\,(v_s - x_s)\,\Gamma_x(x_s) \sum_{j=1}^{N}\sum_{k=1}^{N} a_{ijk}^{(2)}(\delta x_j + \delta x_k), \end{aligned} \tag{16}$$

where $\Gamma_x(x_s)$ is the derivative of the function $\Gamma(x)$ according to x variable in the synchronous manifold (x_s). By substituting $A^{(2)} = K^{(2)} - T$, we have

$$\begin{aligned}\delta\dot{x}_i &= Jf(X_s)\delta X_i - \sigma_1 \sum_{j=1}^{N} L_{ij}^{(1)}\delta x_j - 4\sigma_2\Gamma(x_s)k_i^{(2)}\delta x_i \\ &+ \sigma_2\,(v_s - x_s)\,\Gamma_x(x_s)\left[4k_i^{(2)}\delta x_i - 2\sum_{j=1}^{N} L_{ij}^{(2)}\delta x_j\right]. \end{aligned} \tag{17}$$

Similarly, by considering $L^{(2)} = (N-2)L^{(1)}$, Eq. (18) can be derived as

$$\begin{aligned}\delta\dot{x}_i &= Jf(X_s)\delta X_i - 4\sigma_2\Gamma(x_s)k_i^{(2)}\delta x_i + 4\sigma_2 k_i^{(2)}\,(v_s - x_s)\,\Gamma_x(x_s)\delta x_i \\ &- \left[2\sigma_2\,(v_s - x_s)\,\Gamma_x(x_s)(N-2) + \sigma_1\right]\sum_{j=1}^{N} L_{ij}^{(1)}\delta x_j. \end{aligned} \tag{18}$$

Since $\lambda_i(L^{(1)}) = N$, $i = 2, \ldots, N$, the linearized system whose maximum Lyapunov exponent (Λ) determines the stability of the

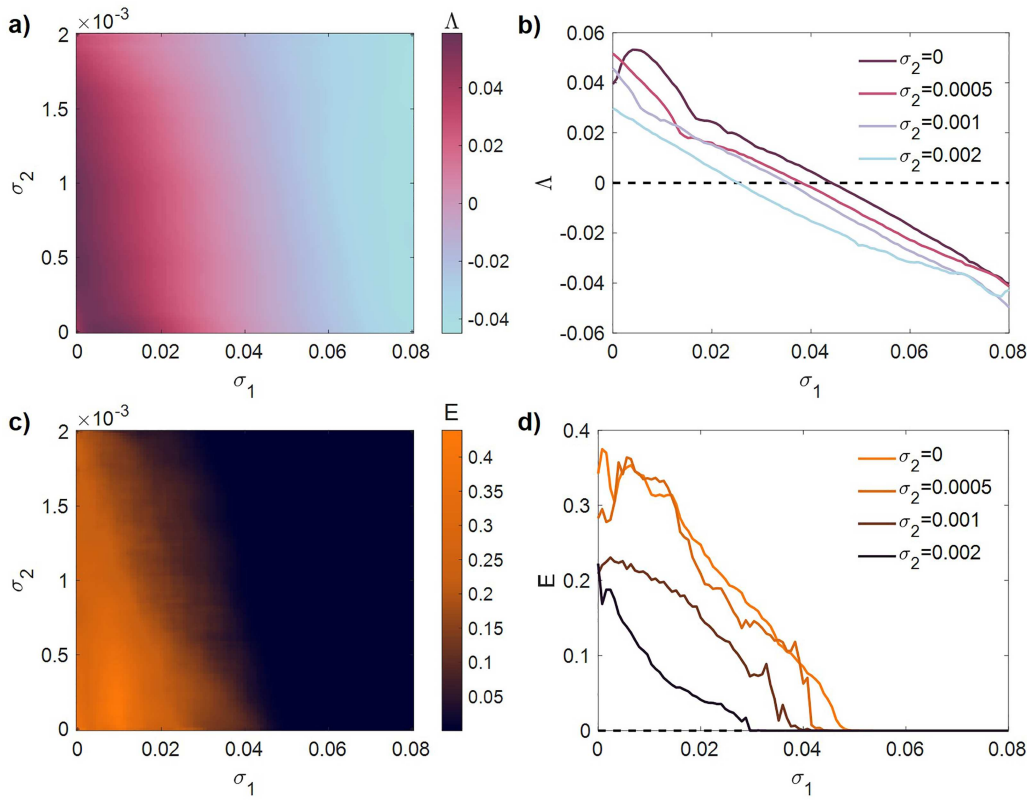

FIG. 7. The regions of synchronous and asynchronous states for $N = 20$ neurons with chemical second-order interactions. First row: the maximum Lyapunov exponent (Λ) of the linearized equation (19). Second row: the synchronization error (E) computed numerically. (a) and (c) 2D representation in the parameter plane (σ_1, σ_2). (b) and (d) 1D representation according to σ_1 for $\sigma_2 = 0, 0.000\,5, 0.001, 0.002$. It can be observed that involving second-order interactions lead to a lower σ_1 needed for synchronization; however, in contrast to the diffusive second-order interactions, the boundary separating two regions is not linear.

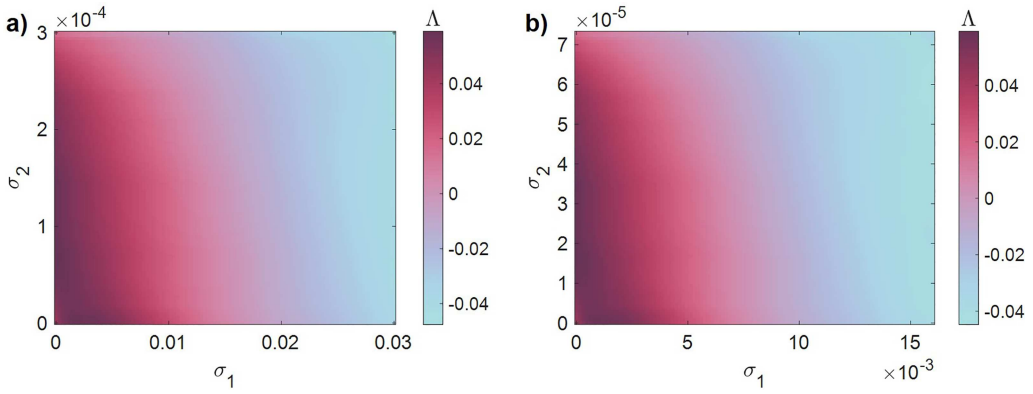

FIG. 8. The maximum Lyapunov exponent (Λ) of the linearized equation (19) for neurons with chemical second-order interactions in the parameter plane (σ_1, σ_2) for $N = 50$ (a) and $N = 100$ (b). The range of coupling strengths decreases by increasing the network size.

synchronization is obtained as follows:

$$\begin{aligned}\dot{\eta}_x &= Jf(X_s)\eta - 4\sigma_2\Gamma(x_s)k_i^{(2)}\eta_x + 4\sigma_2 k_i^{(2)}\,(v_s - x_s)\,\Gamma_x(x_s)\eta_x \\ &\quad\times\left[2\sigma_2\,(v_s - x_s)\,\Gamma_x(x_s)(N-2) + \sigma_1\right]N\eta_x, \\ \dot{\eta}_y &= Jg(X_s)\eta, \\ \dot{\eta}_z &= Jh(X_s)\eta.\end{aligned} \tag{19}$$

Therefore, the synchronization of the network with second-order chemical connections is stable if Λ [Eq. (19)] < 0.

Figure 7 presents the regions of the synchrony and asynchrony by varying the coupling strengths. It can be observed that the required electrical coupling strength decreases with considering the chemical coupling strength. For example, Fig. 7(b) represents that by setting $\sigma_2 = 0.0005$, the synchronization is achieved for $\sigma_1 = 0.044$. By a slight increase in σ_2, more decrease in the electrical coupling strength is seen, such that for $\sigma_2 = 0.002$, the neurons become synchronous at $\sigma_1 = 0.0296$. In contrast to the diffusive coupling, the relation between σ_1 and σ_2 (the border of synchrony and asynchrony) is not linear due to the existence of the nonlinear term in the obtained linearized system [Eq. (19)]. Note that for $\sigma_2 > 0.002$, the synchronous manifold of the neurons changes to the resting state, and the oscillation death appears. Therefore, in our simulations, we have set $0 < \sigma_2 < 0.002$ to consider the oscillating region. The numerically calculated synchronization error, which is illustrated in parts c and d, confirms the results of the linear stability analysis.

Similar to the diffusive coupling, by increasing the number of neurons in the network, the value of coupling strengths for synchronization decreases remarkably. However, the relation between the coupling strengths in the small and larger networks is not as simple and linear as diffusive coupling. The maximum Lyapunov

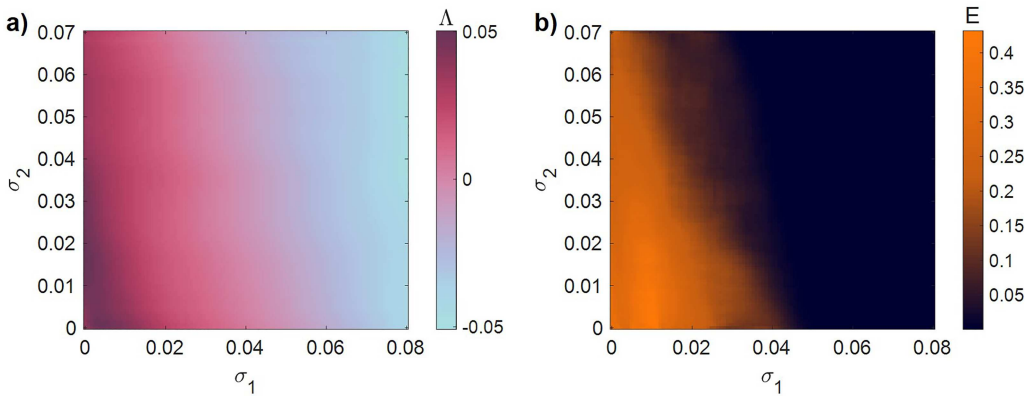

FIG. 9. The regions of synchronous and asynchronous states for $N = 20$ neurons coupled with only pairwise connections through both electrical and chemical synapses. (a) Maximum Lyapunov exponent of the linearized perturbed system. (b) Numerical synchronization error. By increasing σ_2, synchronization occurs in lower σ_1; however, the strength of chemical connections in pairwise coupling is much higher than the second-order ones.

exponent of Eq. (19) for $N = 50$ and $N = 100$ is presented in Fig. 8. The reduced ranges of coupling strengths for $N = 50$ and $N = 100$ are notable in these figures.

Next, we compute the synchronization cost of the chemical second-order interactions and compare with the electrical ones. The synchronization cost is defined the same as Sec. III A, $C_2 = \frac{N(N-1)}{2}(\sigma_1 + (N-2)\sigma_2)$. Since the relation between σ_1 and σ_2 in the synchronization state is nonlinear, we cannot find C_2 analytically. Thus, the cost can be computed numerically by using the σ_1 and σ_2 values obtained from the linear stability analysis. Referring to Fig. 7, one can find that although by adding the chemical second-order interactions a lower σ_1 is needed, $\sigma_1 + (N-2)\sigma_2$ is more than $\sigma_1 = \sigma_{th}$. As a result, the second-order chemical interactions lead to the increment of cost. This is in contrast to the case of electrical second-order coupling. However, second-order chemical connections have lower synchronization costs than first-order chemical connections. To represent this, the following network with electrical and chemical pairwise connections is considered:

$$\begin{aligned} \dot{x}_i &= f(x_i, y_i, z_i) + \sigma_1 \sum_{j=1}^{N} a_{ij}^{(1)}(x_j - x_i) + \sigma_2'(v_s - x_i) \sum_{j=1}^{N} a_{ij}^{(1)} \Gamma(x_j)), \\ \dot{y}_i &= g(x_i, y_i, z_i), \\ \dot{z}_i &= h(x_i, y_i, z_i). \end{aligned} \tag{20}$$

The linear stability analysis of this network has been previously presented in Ref. 16. Figure 9 represents the synchronous and asynchronous regions in the plane of σ_1 and σ_2. It can be observed that by increasing σ_2, the network is synchronized for a lower σ_1. However, the σ_2 values are much higher than those obtained in the network with second-order chemical connections. Similarly, the synchronization cost can be computed by $C_1' = \frac{N(N-1)}{2}(\sigma_1 + \sigma_2')$ numerically with using the threshold values found by the linear stability analysis. The comparison between C_2 and C_1' is achieved by comparing $(N-2)\sigma_2$ and σ_2' for fixed σ_1. Checking the required chemical coupling strength for synchronization in Figs. 7 and 9 represents that $(N-2)\sigma_2 < \sigma_2'$ and, thus, $C_2 < C_1'$. Subsequently, the cost of pairwise chemical connections is higher than the cost of second-order chemical connections.

IV. CONCLUSIONS

This paper studied the synchronization of a simplicial complex of neurons coupled with pairwise and higher-order interactions. It was assumed that the pairwise connections are diffusive electrical synapses. The synchronization was investigated by performing the linear stability analysis and also computing the synchronization error. Two cases were considered for the second-order interactions: (1) linear diffusive coupling and (2) nonlinear chemical coupling. In both cases, it was observed that by adding the second-order interactions even with too weak strength, a lower first-order coupling strength is needed for achieving synchronization. In the linear diffusive second-order interactions, the relation between two coupling strengths for synchronization was linear, and its equation was derived. Furthermore, it was shown that by increasing the number of neurons in the network, the required coupling strengths for synchronization decreased, whereas the decrement in the second-order coupling strength was notable. A synchronization cost was defined based on the coupling strength and the connections. It was shown that in the diffusive second-order interaction, the synchronization cost is smaller than when only the diffusive links are present. Moreover, the cost was reduced by strengthening the second-order coupling. In contrast, adding the second-order chemical interactions resulted in the increment of the cost. However, it was represented that the second-order chemical interactions have a lower cost than when the chemical interactions are defined on the links. Consequently, it can be concluded that the second-order interactions can enhance synchronization by decreasing the cost.

ACKNOWLEDGMENTS

M.P. was supported by the Slovenian Research Agency (Grant Nos. P1-0403 and J1-2457).

AUTHOR DECLARATIONS

Conflict of Interest

The authors have no conflicts of interest to disclose.

DATA AVAILABILITY

Data sharing is not applicable to this article as no new data were created or analyzed in this study.

REFERENCES

[1]D. Ghosh, M. Frasca, A. Rizzo, S. Majhi, S. Rakshit, K. Alfaro-Bittner, and S. Boccaletti, "Synchronization in time-varying networks," arXiv:2109.07618 (2021).
[2]S. Boccaletti, J. Kurths, G. Osipov, D. L. Valladares, and C. S. Zhou, "The synchronization of chaotic systems," Phys. Rep. **366**, 1–101 (2002).
[3]A. Arenas, A. Díaz-Guilera, J. Kurths, Y. Moreno, and C. Zhou, "Synchronization in complex networks," Phys. Rep. **469**, 93–153 (2008).
[4]J. Fell and N. Axmacher, "The role of phase synchronization in memory processes," Nat. Rev. Neurosci. **12**, 105–118 (2011).
[5]Z. Gao, W. Dang, X. Wang, X. Hong, L. Hou, K. Ma, and M. Perc, "Complex networks and deep learning for EEG signal analysis," Cognit. Neurodyn. **15**, 369–388 (2021).
[6]J. D. Touboul, C. Piette, L. Venance, and G. B. Ermentrout, "Noise-induced synchronization and antiresonance in interacting excitable systems: Applications to deep brain stimulation in Parkinson's disease," Phys. Rev. X **10**, 011073 (2020).
[7]S. Pusil, S. I. Dimitriadis, M. E. López, E. Pereda, and F. Maestú, "Aberrant MEG multi-frequency phase temporal synchronization predicts conversion from mild cognitive impairment-to-Alzheimer's disease," NeuroImage **24**, 101972 (2019).
[8]R. Abreu, A. Leal, F. L. da Silva, and P. Figueiredo, "EEG synchronization measures predict epilepsy-related BOLD-FMRI fluctuations better than commonly used univariate metrics," Clin. Neurophysiol. **129**, 618–635 (2018).
[9]Q. Liu, Q. Wang, X. Li, X. Gong, X. Luo, T. Yin, J. Liu, and L. Yi, "Social synchronization during joint attention in children with autism spectrum disorder," Autism Res. **14**, 2120–2130 (2021).
[10]I. Hussain, S. Jafari, D. Ghosh, and M. Perc, "Synchronization and chimeras in a network of photosensitive FitzHugh-Nagumo neurons," Nonlinear Dyn. **104**, 2711–2721 (2021).
[11]I. Hussain, D. Ghosh, and S. Jafari, "Chimera states in a thermosensitive FitzHugh-Nagumo neuronal network," Appl. Math. Comput. **410**, 126461 (2021).
[12]E. Shajan, M. P. Asir, S. Dixit, J. Kurths, and M. D. Shrimali, "Enhanced synchronization due to intermittent noise," New J. Phys. **23**, 112001 (2021).

[13]J. Tang, J. Ma, M. Yi, H. Xia, and X. Yang, "Delay and diversity-induced synchronization transitions in a small-world neuronal network," Phys. Rev. E **83**, 046207 (2011).
[14]A. Bandyopadhyay and S. Kar, "Impact of network structure on synchronization of Hindmarsh-Rose neurons coupled in structured network," Appl. Math. Comput. **333**, 194–212 (2018).
[15]M. Shafiei, F. Parastesh, M. Jalili, S. Jafari, M. Perc, and M. Slavinec, "Effects of partial time delays on synchronization patterns in Izhikevich neuronal networks," Eur. Phys. J. B **92**, 20160216 (2019).
[16]S. Rakshit, B. K. Bera, D. Ghosh, and S. Sinha, "Emergence of synchronization and regularity in firing patterns in time-varying neural hypernetworks," Phys. Rev. E **97**, 052304 (2018).
[17]Z. Wang, F. E. Alsaadi, and V.-T. Pham, "Synchronization in a multilayer neuronal network: Effect of time delays," Eur. Phys. J. Spec. Top. **228**, 2391–2403 (2019).
[18]C. K. Volos, I. Kyprianidis, I. Stouboulos, E. Tlelo-Cuautle, and S. Vaidyanathan, "Memristor: A new concept in synchronization of coupled neuromorphic circuits," J. Eng. Sci. Technol. **8**, 157–173 (2015).
[19]S. Mostaghimi, F. Nazarimehr, S. Jafari, and J. Ma, "Chemical and electrical synapse-modulated dynamical properties of coupled neurons under magnetic flow," Appl. Math. Comput. **348**, 42–56 (2019).
[20]M. Shafiei, S. Jafari, F. Parastesh, M. Ozer, T. Kapitaniak, and M. Perc, "Time delayed chemical synapses and synchronization in multilayer neuronal networks with ephaptic inter-layer coupling," Commun. Nonlinear Sci. Numer. Simul. **84**, 105175 (2020).
[21]A. Salova and R. M. D'Souza, "Cluster synchronization on hypergraphs," arXiv:2101.05464 (2021).
[22]T. Carletti, D. Fanelli, and S. Nicoletti, "Dynamical systems on hypergraphs," J. Phys.: Complexity **1**, 035006 (2020).
[23]C. Bick, E. Gross, H. A. Harrington, and M. T. Schaub, "What are higher-order networks?," arXiv:2104.11329 (2021).
[24]G. Petri, P. Expert, F. Turkheimer, R. Carhart-Harris, D. Nutt, P. J. Hellyer, and F. Vaccarino, "Homological scaffolds of brain functional networks," J. R. Soc. Interface **11**, 20140873 (2014).
[25]L.-D. Lord, P. Expert, H. M. Fernandes, G. Petri, T. J. Van Hartevelt, F. Vaccarino, G. Deco, F. Turkheimer, and M. L. Kringelbach, "Insights into brain architectures from the homological scaffolds of functional connectivity networks," Front. Syst. Neurosci. **10**, 85 (2016).
[26]G. F. de Arruda, M. Tizzani, and Y. Moreno, "Phase transitions and stability of dynamical processes on hypergraphs," Commun. Phys. **4**, 175–308 (2021).
[27]F. Battiston, G. Cencetti, I. Iacopini, V. Latora, M. Lucas, A. Patania, J.-G. Young, and G. Petri, "Networks beyond pairwise interactions: Structure and dynamics," Phys. Rep. **874**, 1–92 (2020).
[28]R. Ghorbanchian, J. G. Restrepo, J. J. Torres, and G. Bianconi, "Higher-order simplicial synchronization of coupled topological signals," Commun. Phys. **4**, 1 (2021).
[29]V. Salnikov, D. Cassese, and R. Lambiotte, "Simplicial complexes and complex systems," Eur. J. Phys. **40**, 014001 (2019).
[30]F. Battiston, E. Amico, A. Barrat, G. Bianconi, G. Ferraz de Arruda, B. Franceschiello, I. Iacopini, S. Kéefi, V. Latora, and Y. Moreno, "The physics of higher-order interactions in complex systems," Nat. Phys. **17**, 1093–1098 (2021).
[31]P. S. Skardal and A. Arenas, "Abrupt desynchronization and extensive multistability in globally coupled oscillator simplexes," Phys. Rev. Lett. **122**, 248301 (2019).
[32]A. P. Millán, J. G. Restrepo, J. J. Torres, and G. Bianconi, "Geometry, topology and simplicial synchronization," arXiv:2105.00943 (2021).
[33]T. Tanaka and T. Aoyagi, "Multistable attractors in a network of phase oscillators with three-body interactions," Phys. Rev. Lett. **106**, 224101 (2011).
[34]P. S. Skardal and A. Arenas, "Memory selection and information switching in oscillator networks with higher-order interactions," J. Phys.: Complexity **2**, 015003 (2020).
[35]A. P. Millán, J. J. Torres, and G. Bianconi, "Explosive higher-order Kuramoto dynamics on simplicial complexes," Phys. Rev. Lett. **124**, 218301 (2020).
[36]P. S. Skardal and A. Arenas, "Higher order interactions in complex networks of phase oscillators promote abrupt synchronization switching," Commun. Phys. **3**, 218 (2020).
[37]M. Lucas, G. Cencetti, and F. Battiston, "Multiorder Laplacian for synchronization in higher-order networks," Phys. Rev. Res. **2**, 033410 (2020).
[38]S. Rakshit, B. K. Bera, E. M. Bollt, and D. Ghosh, "Intralayer synchronization in evolving multiplex hypernetworks: Analytical approach," SIAM J. Appl. Dyn. Syst. **19**, 918–963 (2020).
[39]F. Sorrentino, "Synchronization of hypernetworks of coupled dynamical systems," New J. Phys. **14**, 033035 (2012).
[40]L. V. Gambuzza, F. Di Patti, L. Gallo, S. Lepri, M. Romance, R. Criado, M. Frasca, V. Latora, and S. Boccaletti, "The master stability function for synchronization in simplicial complexes," arXiv:2004.03913 (2020).
[41]A. Tlaie, I. Leyva, and I. Sendiña-Nadal, "High-order couplings in geometric complex networks of neurons," Phys. Rev. E **100**, 052305 (2019).
[42]R. A. A. Ince, F. Montani, E. Arabzadeh, M. E. Diamond, and S. Panzeri, "On the presence of high-order interactions among somatosensory neurons and their effect on information transmission," J. Phys. Conf. Ser. **197**, 012013 (2009).
[43]S.-I. Amari, H. Nakahara, S. Wu, and Y. Sakai, "Synchronous firing and higher-order interactions in neuron pool," Neural Comput. **15**, 127–142 (2003).
[44]M. Dhamala, V. K. Jirsa, and M. Ding, "Transitions to synchrony in coupled bursting neurons," Phys. Rev. Lett. **92**, 028101 (2004).